Simulation of Two-Dimensional Random Structure Through Inversely Generated Delaunay Subgraphs

R. J. Matthews, J. D. Richardson and C. D. Wilson

***Abstract*— Subgraphs taken from Delaunay triangulations are used as a basis for the representation of spacing in two-dimensional random structure. Stochastic simulations are presented in which Delaunay triangulations are used to determine sets of points rather than vice versa. Reversal of the usual triangulation problem allows the simulations to be based on side-length probability distribution functions. A convenient finding is that, for triangulations with a standard deviation of less than or equal to approximately one-half of the minimum spacing, simulations tend to reproduce the original distributions without using conditional probabilities on the generated side lengths. It is also shown that, for distributions of much larger variance, simulations may be readily tuned based on the introduction of an assumed, possibly fictitious, conditional probability for the third side in each triangle. Two distributions are used as numerical examples, one which shows that the scatter in fiber density in carbon-fiber composites can be readily simulated from the data obtained by image-processing of micrographs of ply cross-sections and a second which shows that an arbitrary distribution may be simulated through introduction of the aforementioned assumed conditional probability on the third side in each triangle.**

I. Introduction

The statistical description of spatially random structure plays a key role in simulating many physical phenomena. Often, simulations seek to target rare-event phenomena using Monte Carlo methods so that a large sample population may be required in order to observe a significant number of events. At some level, the required population size of the random structure may exceed that which may be observed experimentally. In such cases, it is attractive if statistically representative random structure may be generated computationally.

In terms of representations of random structure, much literature has been devoted to the problem of close packing of disks, spheres, and even arbitrarily shaped three-dimensional bodies since close packings are observed in many physical instances where particles tend toward potential energy minimization either subject to mutual attraction or under the influence of gravity. While close packings have been studied experimentally [1], [2], for obvious convenience, computer simulation has also been widely used in various investigations [3]–[9]. A general overview for the broad class of random close packings has been given by Stoyan [10]. Various possibilities exist for choosing a suitable statistical measure to characterize spatial variation in close packings and, often, the pair correlation or radial distribution function [1] is used.

Though problems involving close packing will have similarities with developments herein, the focus of the current effort extends to the more general problem of random point location and comparatively larger variations in density. For less densely populated random structure, the overall patterns of the spatial distributions may appear to be homogeneous only at scales which are very large in comparison to a characteristic dimension of the smaller structure. For physical phenomena in which the system response will depend on structural density over a range of scales, the ability to describe and model the heterogeneous nature of density over these scales is important. An example of a system with such a dependence would be carbon fiber composites where elastic constants at a component level depend on effective carbon fiber density at component length scales, whereas failure from micro-cracking could show crack initiation dependence on fiber packing at a much smaller scale.

Statistical measures used to describe random structures of densities too low to be considered as close packings also include the aforementioned use of the pair correlation function which has been used in characterization of cloud droplets [11] and for the distribution of plants in an arid environment [12]. Additionally, Ripley's K-function is often applied as a statistical measure and has been used, for example, to characterize clustering of archaeological sites [13] as well as to investigate particular clustering of bald cypress trees among other species of trees growing in a swamp environment [14].

The method to be presented here will involve stochastic tessellations based on target statistical measures taken from subgraphs of Delaunay triangulations. Delaunay triangulations and their dual, Voronoi tessellations, are often used in simulations of random structure. However, their historic use and their use in the current work differ considerably. The computational problem most widely considered in Delaunay triangulations is the standard problem of construction [15]–[22], namely, given a set of points, determine its Delaunay triangulation. For reference, a second common problem is the point (vertex) location problem within an existing triangulation [23], [24] which seeks to locate a given point in terms of a path along triangle edges and should not be confused with directly placing points into a Euclidean space of the given problem dimensionality.

Robert J. Matthews was formerly a graduate student in the Department of Mechanical Engineering at Tennessee Tech University, Cookeville, TN USA 38505 and currently is Director of Research for Covenant Capital Management, Nashville, TN 37203.

Joseph D. Richardson was formerly an Associate Professor of Mechanical Engineering at Tennessee Tech University, Cookeville, TN USA 38505 and is currently an Assistant Professor of Mechanical Engineering at the University of South Alabama, Mobile, AL USA 36688. Corresponding author: *jdrichardson@southalabama.edu*

Christopher D. Wilson is an Associate Professor of Mechanical Engineering at Tennessee Tech University, Cookeville, TN USA 35805.

The point location method described here differs from previous usage of Delaunay triangulations in that simulation of point locations in space is through the triangulation itself using a statistical description of the individual triangles taken to match Delaunay subgraphs of some target random structure. The method is particularly attractive when image processing software can be used to compute Delaunay triangulations of sample populations along with a record of the individual triangles in the sets. Once the geometric statistics of the triangulation are known, the standard Delaunay triangulation problem is reversed in the sense that the triangulation may be simulated under the appropriate rules for Delaunay triangulations in order to locate the individual points in the sets. In so doing, the statistics of the triangle side lengths are readily incorporated into the simulations. Since the Delaunay triangulation is unique for a given set of points, aside for some very specific exceptions involving collinearity, it is suggested that representative point fields can be compared for statistical similarity based on the distributions in the triangle side lengths.

The method outlined has been developed primarily for the specific case of carbon fiber dispersions in a phenolic matrix and should add to previous work on modeling the stochastic nature of elastic constants in carbon fiber composites [25]–[27]. However, it is suggested and shown that the approach may be used more generally. Of particular interest in the aforementioned case of carbon fiber dispersion is the suggestion that the triangulation rules seem to act as conditional probability 'filters' so that statistically representative sets may be generated without the use of conditional probabilities which may be quite difficult to determine, so long as the variance in the triangle side length distributions is not too great. A second example based on a fictitiously assumed lognormal distribution suggests that, while the consideration of conditional probabilities is necessary for triangulation subgraphs with sufficiently large side length variance, the introduction of fictitious conditional probabilities, perhaps on a single side, may be introduced in order to tune the statistics of the simulated side length data. While very strong statistical similarity was demonstrated herein through informal numerical experimentation with statistical parameters, it is suggested that the approach could be used in conjunction with an optimization scheme based on seeking a quantile-quantile plot of unit slope. It is further suggested that the conditional probabilities could be expressed in terms of numerical cumulative distribution function tables where the table data is obtained from the optimization scheme, though such formalism is not presented here.

The next section gives a brief overview of the Delaunay triangulation and includes some background on the statistics of the carbon fiber dispersions and the methods used to obtain them. Following that, Section III will present the results from Monte Carlo simulations of the given carbon fiber samples along with the second aforementioned fictitious target example.

II. Delaunay Triangulation: Definition and Simulation

The Delaunay triangulation of a set of points is the triangular covering taken from the placement of triangle vertices on the points subject to the constraint that none of the triangles have vertices which are interior to any of the circles circumscribed by any of the other triangles. An example of a portion of a sample triangulation which was taken from simulations based on the first of two numerical examples to be presented later is shown in Figure 1 and includes, in addition to the triangles, their circumscribed circles. Since the triangulation rule prohibits interior triangle vertices, the vertices are located at the intersection of circumscribing circles as may be seen. A commonly-used coverage related to the Delaunay triangulation is the Voronoi tessellation in which the Voronoi polygons are formed from the intersections of the perpendicular bisectors of the triangle sides in the Delaunay triangulation.

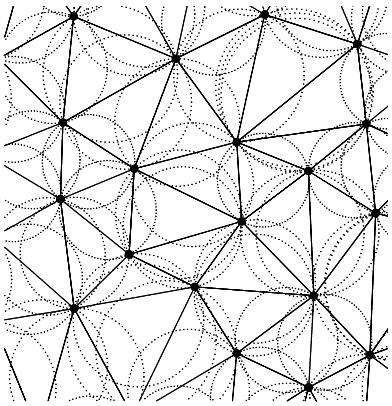

Fig. 1. Portion of a Delaunay triangulation of a set of points.

Aside from some specific instances such as the case when three points are collinear, the Delaunay triangulation is unique for a given set of points. Though unlikely, the case of collinear points may arise in image-processing when only discrete length measures are available; the likelihood of collinear points in double precision simulations is negligible. Based on the uniqueness of the Delaunay triangulation for most point sets taken from real data then, the present approach targets statistical similarity in the spatial distributions of point sets on the basis of statistical similarity in their Delaunay triangulations.

Following considerable numerical experimentation, the random variables chosen for the three degrees of freedom of a triangle in the present investigation were the individual side lengths. One attractive feature regarding the use of lengths is that the tendency toward clustering and rarefaction is at least qualitatively observed from the variance in the side length data. However, the choice to use side lengths, as opposed to angles, was based on superior numerical results observed in initial testing of the approach. In general, the use of angles more naturally introduces conditional probabilities which were more difficult to accurately estimate. For example, for the case of the observed physical data to be described later, an attempt was made to develop the conditional probability of an included angle given two sides in which the parameters of the conditional probability were taken as functions of the two sides. Even though the sample size was on the order of 10^4, it was found that the data was too sparse in many areas and no form was found for the conditional probability which reasonably described the angle over any appreciable range. Fortunately, it was found that the method can work well without the requirement for conditional probabilities estimated from data. For relatively low variance in the side length data, as seen in the physical example, simulations seem to do well without the use of any conditional probabilities, noting that the various constraints imposed in building the triangulation serve as filters on admissibility of side length combinations. For cases involving larger variance in the side length data, it was also found that the simulations are very sensitive to assumed, or fictitious, conditional probabilities introduced for one of the sides, making the simulations readily 'tunable' and

thus obviating the difficult task of estimation of conditional probabilities from data.

A general outline of the simulation used in the present case is given as the following series of steps.

1) A statistical model for triangle side length data of Delaunay triangulations is developed, perhaps either from image analysis data or as a design target. In many instances, the distributions will involve a minimum separation, such as one fiber diameter in the case of carbon fiber composite simulations.
2) A seed random triangle is generated with each side based on three independent observations of a uniform random variable which is mapped onto the triangle side length cumulative distribution function (CDF). If the triangle fails to satisfy the triangle inequality, the sides are all discarded and three new random sides are generated.
3) The triangulation is then extended outward, building on each triangle which has an unshared side while tracking the 'availability' of each side of all triangles in the simulation. For each unshared side, two random instances of side lengths are generated in an attempt to build a new triangle. The CDFs of the two sides, may in general, be taken to depend upon the original unshared side as well as upon one another. The combination of sides and the attendant new vertex location is then evaluated based upon the following ordered criteria:
   a) the triangle inequality,
   b) proximity of the new vertex to previously existing vertices,
   c) and the Delaunay constraint that no vertex falls inside the circumscribing circle of any other triangle.
4) Based on the previous criteria, the following action is taken:
   a) If the two newly generated sides along with the original unshared side fail to satisfy the triangle inequality 3a, the two new sides are discarded and two new independent side lengths are generated.
   b) Following admissibility based on 3a, condition 3b is then considered. One of three actions is taken:
      i) If the minimum distance between the new vertex and the nearest previously existing vertex is less than some small arbitrary factor, taken as 0.1 of the minimum spacing in the present case, a merger of the new vertex onto its closest neighbor is attempted. The merger is conditional in that the previously existing triangle which includes the merger vertex and a shared common vertex is currently available to share the relevant side with a new triangle.
      ii) If a vertex merger is not possible and the minimum distance from the previous item is less than some natural minimum, *e.g.*, one fiber diameter in the case of carbon fiber composites, the sides are rejected and two new sides are generated.
      iii) Otherwise, if no merger could occur and if the new vertex is sufficiently far from all previously existing vertices, vertex placement is accepted subject to the last and final constraint.
   c) The center and radius of the circumscribed circle for each new triangle is determined from the intersection of perpendicular bisectors. Based on 3c, if the new vertex lies inside of any previously existing circumscribed circles or if the circumscribing circle from the new triangle has any previously existing vertices in its interior, the vertex placement is rejected and two new sides are generated.
5) The triangulation is halted after either a preset number of triangles are formed or the simulation is self-arrested as, after a large number of attempts, perhaps 10^7, no new vertex location may be determined for the lowest ordered unshared side in the triangulation.

Obviously, the approach outlined here is only one of many variations which could be developed for successful Monte Carlo simulations of Delaunay triangulation and others could be explored. Perhaps most notably, the present approach makes no attempt to restart a self-arrested pattern, either by clearing or by attempting a flip of two triangles. Such attempts would likely be necessary if triangulation patterns were required which contained $\mathcal{O}(10^3)$ triangles or more; the allowance for self-arrest will be shown to work well for patterns of $\mathcal{O}(10^2)$ triangles. Numerical results are presented in the following section which show that the simulated triangulations are statistically similar either to the physical data sets which were targeted for simulation or, following some experimentation, to an arbitrary distribution taken as a target for simulated patterns.

III. Numerical Examples

Two numerical examples are presented which demonstrate the ability of the approach to model randomness in two-dimensional structure. The first example is based on a series of micrographs of cross-sections of carbon fiber composite samples. Since significant commonality is expected for simulations of many types of two-dimensional problems, a general overview of the entire modeling process, including some background on the image analysis which was used, is given in the next section. A second example will show how the method may be extended to structure with more highly irregular spacing.

A. Random Arrays of Carbon Fibers

It is expected that the scatter in fatigue life data in carbon fiber composites may be attributed in part to the general scatter in fiber distributions as shown in Figure 2 which shows rather extreme cases of packing density variation among cross-section samples of panels which were manufactured under relatively similar conditions.

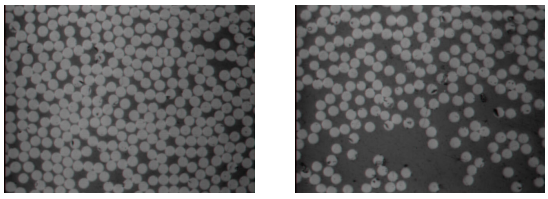

Fig. 2. Variation in fiber distributions within a set of composite panels.

The particular case of cylindrical carbon fibers of uniform size is quite convenient for image processing since the fibers all appear as circles in a cross-sectional view. It is suggested that the general method used here for image processing could be extended either to uniform objects of arbitrary shape which share a common orientation or to arbitrarily oriented objects

which might be well-approximated by an axisymmetric representation.

For the current effort, the software package MATLAB® was used for the physical specimens, both for image-processing and triangulation of the observed samples. A number of samples were prepared and stored as digital images which were then cast into binary intensity fields of black and white pixels, giving images such as the one shown on the left of Figure 3. A single fiber template as shown on the right of Figure 3

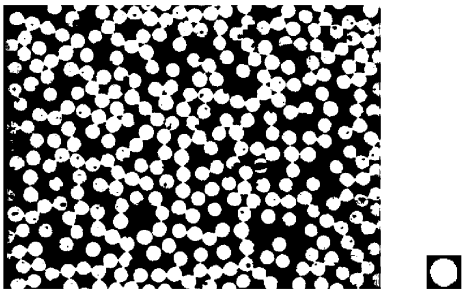

(a) (b)

Fig. 3. (a) Binary image of fibers. (b) Single fiber template (not to scale).

was isolated and used to locate fiber centroids through cross-correlation [28]. An example of the digital image following cross-correlation is shown on the left of Figure 4 where the centroids appear within the brightest areas. After erosion of the image shown on the left, the fiber centroid locations remain as bright spots as shown on the right of Figure 4.

Following the location of the fiber centroids, the images were tessellated with their Delaunay triangulations as shown in Figure 5 using the centroids as the point fields. As can be seen in the figure, the image boundaries create some triangles which are not representative of the interior portion of the triangulation. These outer triangles were excluded from consideration and the remaining triangle side length data was recorded for the samples.

Close examination of Figure 5 shows that the method is generally quite accurate in locating fiber centroids, though fibers may be occasionally missed. Undetected fibers often involve cases where the fibers have surface damage which was not removed through polishing as can be seen in two instances near the upper right corner of the figure. Occasionally, fibers may be missed either when their edges appear to be blurry or when either their size or shape differ sufficiently from the template, as can be observed, for example in the upper right quadrant of the figure, in one instance near the corner and, in another, closer to the center of the image. One may also refer back to the black and white representation of this image shown previously on the left of Figure 3 to see how a few of the fibers were likely to have been missed prior to cross-correlation and erosion.

The logarithm of the amount by which the triangulation side length data in the sample set exceeds its minimum of one fiber diameter was plotted on normal probability axes as shown in Figure 6. The probability plot shows two linear regions which suggests the presence of two sub-populations, each of which could be approximated as lognormal. Attempts to fit the data with a random blend of two different lognormal populations was reasonably successful in terms of matching the data on a quantile-quantile basis. The means from the two distributions

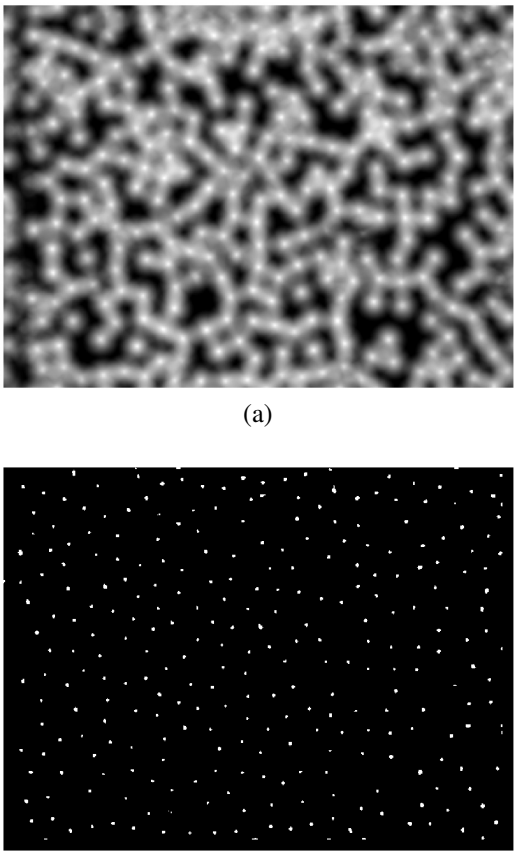

(a)

(b)

Fig. 4. (a) Binary image following cross-correlation. (b) Final determination of centroids by high-threshold erosion.

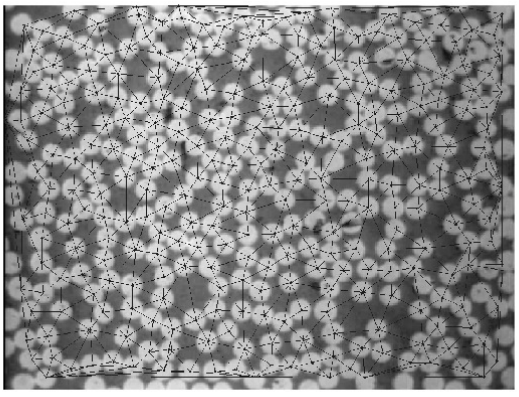

Fig. 5. Cross-section of fibers overlaid with Delaunay triangulation.

which represented the best fit attained for the data were notably separated; an interpretation would be that one population was associated with fibers which were from a closely-packed region while the second was associated with fibers from a region which was comparatively richer in the phenolic resin. For reference, when the data is normalized to a fiber diameter of unity, the measured population has a mean of approximately 1.47 and a standard deviation of 0.412.

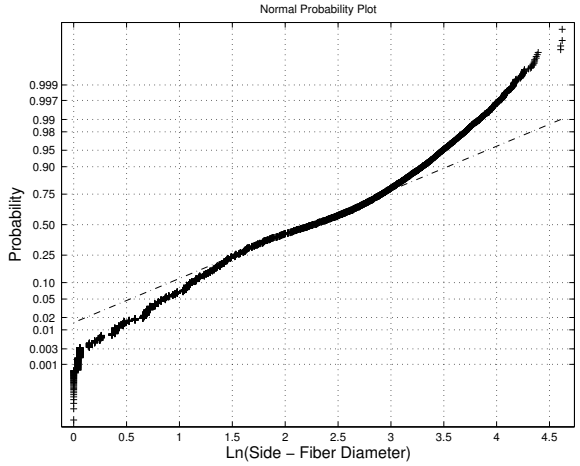

Fig. 6. Logarithm of triangle side length data plotted on normal probability axes.

The present approach is based on Monte Carlo simulations for which there is no clear advantage to the use of closed form expressions for the distribution. The cumulative density function (CDF) of the data was discretized into 200 bins between one fiber diameter and the maximum observed in the data which was approximately 5.02 fiber diameters. A plot of the discretized CDF of the data is shown in Figure 7. In the

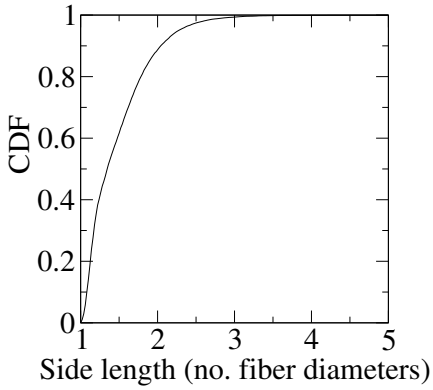

Fig. 7. Discretized CDF for measured triangle side lengths (200 uniform bins).

present study, the public-domain package Grace was used to output the CDF data. The data was set as two Fortran data structures using formatted write statements to produce a CDF table routine using linear interpolation. Due to the sparseness near the tail of the distribution, exactly 50 of the bins were collapsed as the value of the CDF did not increment over them.

A sample population for the simulated data was generated from two hundred tessellation patterns. Each simulation was halted either after 300 triangles were generated or after self-arrest of the triangulation. The side-length counting scheme which was used was chosen to be consistent with the most straightforward counting scheme used to sort the observed data from the micrographs, namely that three sides were counted for each triangle. As such, it should be noted that, both for the simulations and the observed data, shared interior sides were counted twice in the counting scheme while boundary sides were counted once. For consistency, each of the simulations was targeted to have a comparable number of fibers as seen in a typical micrograph.

Sixty of the 200 simulations were halted by the 300 triangle maximum criterion and the average simulation size was approximately 189 triangles. The number of triangle sides counted in the simulations was 113,475 while the observed data had 64779 sides. The generation of possible sides for the construction of new triangles in the Monte Carlo method was based on an unconditional probability for each side with each side based on the CDF shown in Figure 7. Specific consideration was given to ensure that the quasi-random sequence of uniformly random numbers would appear to be non-Markovian to ensure that there was no statistical bias toward, for example, long side–short side combinations, short side–short side combinations, etc. The random number generator used for this project was a decimal implementation of a two-stream, 100 card nonlinear generator as described in [29].

The numerical results from the first example simulation just described are now presented. A comparison of the probability densities for the observed and simulated data is shown on the left of Figure 8. The probability density functions show very strong general agreement, though the PDF from the simulated data is slightly under-valued at the first peak and slightly over-valued at the second, less pronounced, peak. While an overlay of the PDF plots provides a qualitative statistical assessment, a plot of quantiles generally gives a better indication of statistical similarity in two data sets. The quantile-quantile plot on the right of Figure 8 shows that the method produced reasonable statistical similarity in the side-length data from the Delaunay triangulations. Since, for this simulation, all possible side lengths were based on the common CDF shown previously in Figure 7, this example suggests that, for triangulations with relatively low side-length variation, the Delaunay triangulation constraints along with the triangle inequality, serve as an effective conditional probability filters. The attractive feature is that, again for cases in which the random structure shows sufficiently small density variations within the region of interest, the use of conditional probabilities for each triangle to be generated, based on either previously existing sides or angles, may be avoided.

Finally, for this example, a representative pattern from the simulations is shown on the left side of Figure 9. The pattern may be informally compared with the micrographs previously shown in Figure 2 and may also be used to provide a sense of the level of density variations which might conceivably be simulated without the use of conditional probabilities. The right side of Figure 9 shows the Delaunay subgraph used to locate the fibers shown on the left side of the figure.

B. Tuned Simulation of Fictitious Data

In the previous example, it was found that the simulated triangulations produced side-length statistics which were similar to the distribution from which each of the input sides was drawn in the Monte Carlo simulations without the consideration of any conditional probabilities on either one or two of the previously existing sides. However, through numerical experimentation based on other distributions, it was found that, for higher variance in the side-length statistics, the simulations would not reproduce the input statistics when using triangle side lengths which were uncorrelated. Motivation for the second example, then, lies in the assessment of the approach for simulating more general random point sets including those with larger sample variance. In this second example, a fictitious

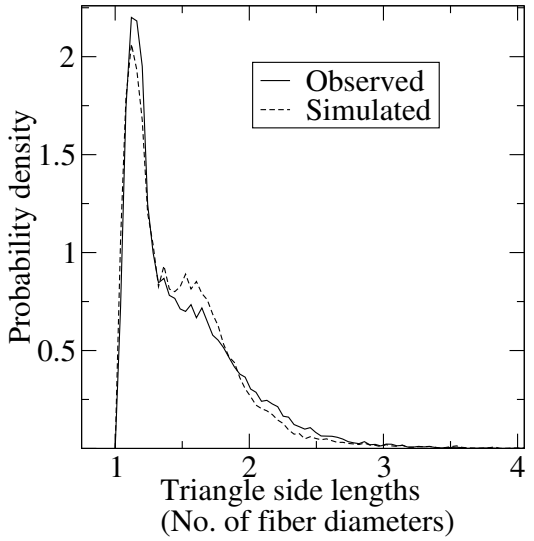

(a)

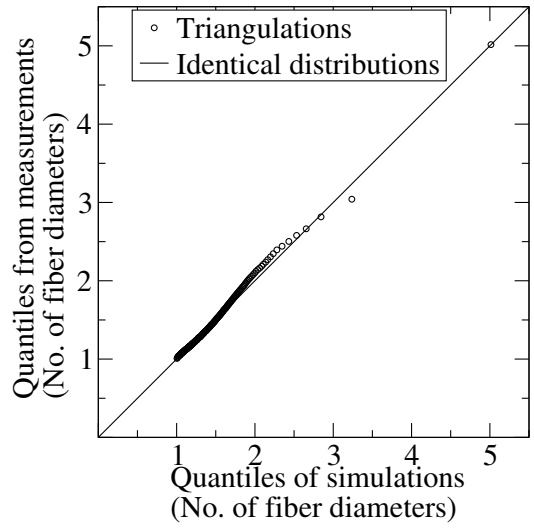

(b)

Fig. 8. (a) Side length histogram comparison. Simulation: 1.13×10^5 samples. Data: 6.5×10^4 samples. (b) Quantile-quantile plot of observed and simulated triangulation side lengths.

distribution is sought based on a lognormal population which, when normalized to unit minimum spacing, has a mean and standard deviation approximately given by 2.45 and 2.06, respectively. While the choice of this particular distribution was somewhat arbitrary, the targeted distribution shows a fivefold increase in the standard deviation of the side lengths of the triangulations in comparison to the previous example population.

For this problem, the quantile-quantile plots are shown in Figure 10 for three different side generation schemes including,

1) The generation of two uncorrelated sides for the second and third sides of each new triangle, each taken from the lognormal population.
2) The generation of an uncorrelated second side from the lognormal population followed by a third side which was taken as uniformly random over the range of lengths specified by the triangle inequality based on the first two sides.
3) The generation of an uncorrelated second side from the lognormal population followed by a third side taken as normally distributed with a mean given as the geometric mean of the first two sides and a standard deviation taken as 0.6 times the allowable range of third sides based on the triangle inequality.

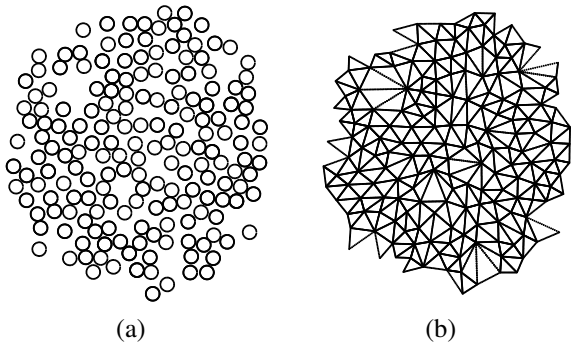

(a) (b)

Fig. 9. (a) Representative plot of random fiber distribution from simulation of carbon fibers. (b) Plot of Delaunay triangulation subgraph for fibers shown on left.

The first scheme above is obviously similar to the previous numerical example while the second two schemes represent attempts to effectively tune the side length statistics to the target distribution. Since the larger side length variation increased the likelihood of early self-arrest, the number of simulations was doubled to 400 and triangulations were rejected if they had less than 125 triangles. It was informally observed, however, that the inclusion of all triangulations regardless of size made only slight differences in the appearances of the various quantile-quantile plots.

While further attention will be given to the successful third scheme, it is most notable from the plot on the left of Figure 10 that the triangle side lengths distributions are highly sensitive to the input statistics of either of the two new sides. As such, it is suggested that a formal optimization of the quantile-quantile plots could easily be developed using a conditional numerical table for the third side CDF.

In spite of the fact that only limited trial and error testing was used, the quantile-quantile plot on the right of Figure 10 shows that an excellent fit of the target distribution was obtained. The highest quantile shown in the plot is the 0.995 quantile. The 100^{th} percentile for the simulated data is not shown due to scaling in the plot since it is at approximately 82 fiber diameters, but, from the connecting line, one can see that the slope, even at the extreme tail, is not too far from unity. For reference, the 100^{th} percentile in the target simulation was taken as the maximum value seen in 10^5 random lengths drawn numerically from the target lognormal distribution. Also for reference, the data set shown for the tuned scheme contains 82,818 triangles.

The probability density functions for the lognormal population of side lengths serving as the target of the simulations and the side lengths from the actual simulations from the tuned scheme 3 are shown in Figure 11. As in the previous example, the simulated data slightly underestimates the target PDF near its peak, but otherwise generally shows very strong agreement with the target PDF. The PDF plot was not even

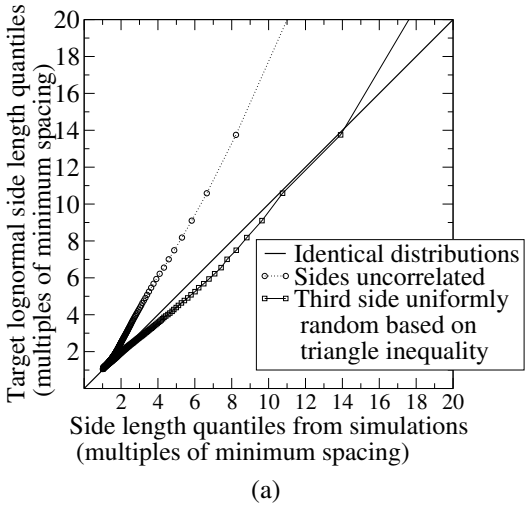

(a)

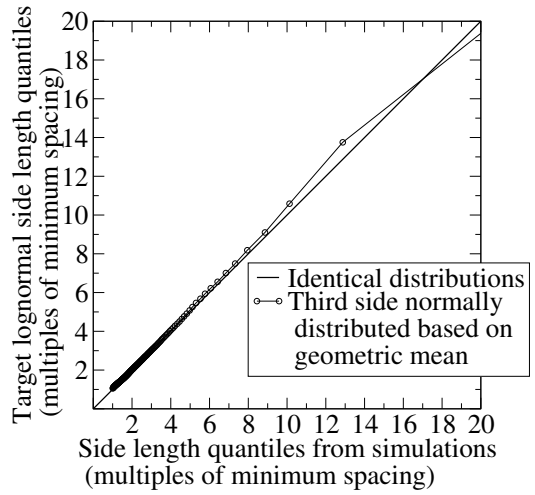

(b)

Fig. 10. (a) Quantile-quantile plot of target lognormal population and simulations with both uncorrelated and uniformly random third side probabilities, (b) Quantile-quantile plot of lognormal population and tuned third side probability.

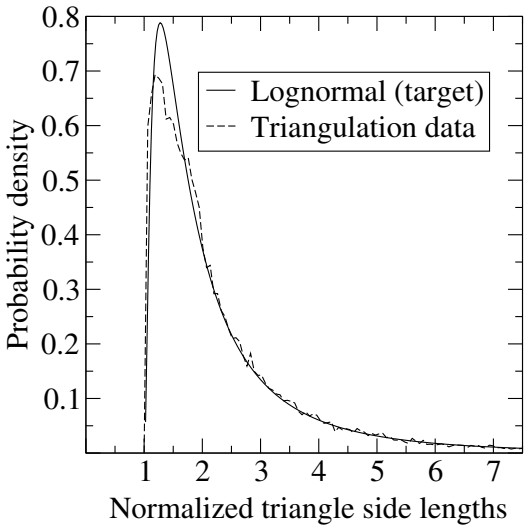

Fig. 11. Comparison of target and tuned simulated triangulation PDFs (approximately 8.28×10^4 samples in simulated set).

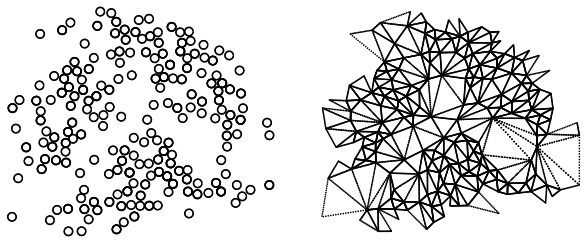

(a) (b)

Fig. 12. (a) Representative point set shown with circles indicating minimum spacing distance, (b) Delaunay triangulation subgraph of the same point set.

viewed until after a suitable third side conditional probability was determined; the informal trial and error tuning of the third side probability was solely on the basis of the quantile-quantile line.

Finally, a representative set of points from the tuned simulation is shown on the left of Figure 12 along with its Delaunay subgraph shown on the right. The circles in the figure indicate the minimum spacing. The pattern shown provides visual indication of the types of spacing irregularities associated with the target distribution in this example and may suggest other types of random structure which might be well simulated with this approach.

IV. Conclusions

The side length statistics from subgraphs taken from Delaunay triangulations were used to represent the spatial randomness in a two-dimensional field. Random Delaunay subgraphs were built using a Monte Carlo method and, on the basis of statistical similarity in the side length probability density functions, were shown to be similar to one target taken from physical data as well as another target based on arbitrarily assumed fictitious data. Though not addressed herein, the present approach could be easily modified to model its companion tessellation based on Voronoi polygons, often used in polycrystalline simulations as in the case of random grain orientations in metallurgical simulations. Though also not considered, it is further suggested that the method could be extended to three-dimensional fields.

A first example was based on the Delaunay statistics from a series of micrographs taken of carbon fiber composite cross sections which were used to form a numerical cumulative distribution function (CDF). The field of fibers had a mean of 1.47 times the fiber radius and a standard deviation of 0.412 fiber diameters. An interesting and convenient finding is that, for this level of scatter, all triangle side lengths can apparently be taken as uncorrelated based on the same measured distribution. In so doing, the fields generated from the Monte Carlo method tended to reproduce the observed input statistics in terms of side length data. While somewhat surprising, it is noted that, to some extent, the triangle inequality and the Delaunay criteria act as conditional probability filters as certain possible combinations drawn from the random pool were culled

on these bases.

A second example considered an arbitrary target lognormal distribution with mean and standard deviation of 2.45 and 2.06 times the minimum separation distance, respectively. It is noted that the target in the second example had a standard deviation which presented a fivefold increase over the first example. Perhaps the most important finding from the second example is that, while conditional probabilities cannot be avoided for fields showing greater variance in spacing, simulations based on the proposed method exhibit a high level of 'tunability' based on an assumed conditional probability on the third side in each triangle. This tunability is based on seeking a slope of unity for the quantile-quantile lines between simulations and target. For the given problem, the third side was taken as normally distributed about the geometric mean of the other two sides. Excellent agreement between the simulations and their target, both in terms of the quantile-quantile line and the appearance of their probability density functions, was obtained by informal experimentation with the standard deviation in the assumed form for the third side distribution in terms of its range specified by the triangle inequality. The sensitivity of the shape of the quantile-quantile curve to the input statistics of just one of the sides in the triangulation suggests that the proposed approach could be readily modified to include a formal optimization procedure, conceivably using a discretized numerical CDF for the third side.

V. Acknowledgments

This work was supported by the National Center for Advanced Manufacturing under grant number NCC8-233. Additionally, the authors acknowledge computational support from the Center for Manufacturing Research, an Accomplished Center of Excellence supported by the State of Tennessee and located at Tennessee Technological University. The corresponding author would also like to acknowledge some valuable discussions with J. A. N. Napier of the Chamber of Mines Research Organisation, South Africa.

References

[1] A. Panaitescu and A. Kudrolli, "Spatial distribution functions of random packed granular spheres obtained by direct particle imaging," *Physical Review E*, vol. 81, p. 060301, 2010.

[2] S. Mukhopadhyay and J. Peixinho, "Packings of deformable spheres," *Physical Review E*, vol. 84, p. 011302, 2011.

[3] A. Bezrukov, D. Stoyan, and M. Bargieł, "Spatial statistics for simulated packings of spheres," *Image Analysis & Stereology*, vol. 20, pp. 203–206, 2001.

[4] D. He, N. N. Ekere, and L. Cai, "Two-dimensional percolation and cluster structure of the random packing of binary disks," *Physical Review E*, vol. 65, p. 061304, 2002.

[5] Y. T. Feng, K. Han, and D. R. J. Owen, "Filling domains with disks: an advancing front approach," *International Journal for Numerical Methods in Engineering*, vol. 56, pp. 699–713, 2003.

[6] J. Zhou, Y. Zhang, and J. K. Chen, "Numerical simulation of random packing of spherical particles for powder-based additive manufacturing," *Journal of Manufacturing Science and Engineering*, vol. 131, p. 031004, 2009.

[7] Y. Jiao, F. H. Stillinger, and S. Torquato, "Distinctive features arising in maximally random jammed packings of superballs," *Physical Review E*, vol. 81, p. 041304, 2010.

[8] R. D. Batten, F. H. Stillinger, and S. Torquato, "Inherent structures for soft long-range interactions in two-dimensional many-particle systems," *The Journal of Chemical Physics*, vol. 135, p. 054104, 2011.

[9] Y. Jiao, F. H. Stillinger, and S. Torquato, "Nonuniversality of density and disorder in jammed sphere packings," *Journal of Applied Physics*, vol. 109, p. 013508, 2011.

[10] D. Stoyan, "Random systems of hard particles: Models and statistics," *Chinese Journal of Stereology and Image Analysis*, vol. 7, pp. 1–14, 2002.

[11] R. A. Shaw, A. B. Kostinski, and M. L. Larsen, "Towards quantifying droplet clustering in clouds," *Quarterly Journal of the Royal Meterological Society*, vol. 128, pp. 1043–1057, 2002.

[12] T. Wiegand, W. D. Kissling, P. A. Cipriotti, and M. R. Aguiar, "Extending point pattern analysis for objects of finite size and irregular shape," *Journal of Ecology*, vol. 94, pp. 825–837, 2006.

[13] A. Bevan and J. Conolly, "Multiscalar approaches to settlement pattern analysis," in *Confronting Scale in Archaeology: Issues of Theory and Practice*, pp. 217–234, 2006.

[14] P. M. Dixon, "Ripley's K function," in *Encyclopedia of Environmentrics*, pp. 1796–1803, John Wiley & Sons, Ltd, 2002.

[15] C. Du, "An algorithm for automatic Delaunay triangulation of arbitrary planar domains," *Advances in Engineering Software*, vol. 27, pp. 21–26, 1996.

[16] P. Su and R. L. S. Drysdale, "A comparison of sequential Delaunay triangulation algorithms," *Computational Geometry*, vol. 7, pp. 361–385, 1997.

[17] P. Cignoni, C. Montani, and R. Scopigno, "Dewall: A fast divide and conquer Delaunay triangulation algorithm in E^d," *Computer-Aided Design*, vol. 30, pp. 333–341, 1998.

[18] B. Žalik, "An efficient sweep-line Delaunay triangulation algorithm," *Computer-Aided Design*, vol. 37, pp. 1027–1038, 2005.

[19] Ø. Hjelle and M. Dæhlen, *Triangulations and Applications*. Springer, 2006.

[20] J.-D. Boissonnat, O. Devillers, and S. Hornus, "Incremental construction of the Delaunay triangulation and the Delaunay graph in medium dimension," in *SCG '09: Proceedings of the 25th annual symposium on computational geometry*, Association for Computing Machinery, 2009.

[21] A. Biniaz and G. Dastghaibyfard, "A faster circle-sweep Delaunay triangulation algorithm," *Advances in Engineering Software*, vol. 43, pp. 1–13, 2012.

[22] S. H. Lo, "Delaunay triangulation of non-uniform point distributions by means of multi-grid insertion," *Finite Elements in Analysis and Design*, vol. 63, pp. 8–22, 2013.

[23] E. P. Mücke, I. Saias, and B. Zhu, "Fast randomized point location without preprocessing in two- and three-dimensional Delaunay triangulations," *Computational Geometry*, vol. 12, 1999.

[24] P. M. M. de Castro and O. Devillers, "Simple and efficient distribution-sensitive point location in triangulations," in *SIAM Workshop on Algorithm Engineering and Experiments*, pp. 127–138, 2011.

[25] P. J. Hine, H. R. Lusti, and A. A. Gusev, "Numerical simulation of the effects of volume fraction, aspect ratio and fibre length distribution on the elastic and thermoelastic properties of short fibre composites," *Composites Science and Technology*, vol. 62, pp. 1445–1453, 2002.

[26] V. A. Buryachenko, N. J. Pagano, R. Y. Kim, and J. E. Spowart, "Quantitative description and numerical simulation of random microstructures of composites and their effective elastic moduli," *International Journal of Solids and Structures*, vol. 40, pp. 47–72, 2003.

[27] M. Gangadhar and M. W. Zehn, "A methodology to model spatially distributed uncertainties in thin-walled structures," *ZAMM-Journal of Applied Mathematics and Mechanics*, vol. 87, pp. 360–376, 2007.

[28] G. A. Baxes, *Digital Image Processing: Principles and Applications*. J. Wiley & Sons, 1994.

[29] J. D. Richardson, "Nonlinear pseudo random number generation using digit isolation and entropy buffers," (submitted for publication).